PERSONALIZED HEAD-RELATED TRANSFER FUNCTION MEASUREMENT FOR ACOUSTIC VIRTUAL REALITY DEVELOPMENT

Zoltan HARASZY[1]

Conceptul de Realitate Acustică Virtuală este frecvent folosit ca interfață om-maşină în asistarea persoanelor nevăzătoare. Implementarea practică se bazează pe funcțiile Head-Related Transfer Function, denumite funcții HRTF. În această lucrare sunt prezentate detaliile unei proceduri de măsurare ale acestor funcții HRTF pentru o singură persoană într-un mediu aproape fără ecouri. Sunt prezentate: locul de desfăşurare, proiectarea semnalului de test, respectiv post-procesarea semnalului înregistrat pentru extragerea funcțiilor HRTF. Aceste funcții vor fi folosite pentru implementarea unui mediu acustic virtual pentru persoana în cauză.

The Acoustical Virtual Reality concept is often used as man-machine interface in electronic travel aids for the blind. The implementation is based on the Head-Related Transfer Functions (HRTFs). We describe the details of an experimental HRTF measurement procedure for measuring the HRTFs for one single subject in a near anechoic environment. We present the measurement facility, the design of the test signal, and the post-processing of the measured raw acoustic signals to extract the HRTFs. The post-processing includes the equalization of the used hardware. The obtained personalized HRTFs will be used to generate a virtual audio environment for the subject.

Keywords: head related transfer functions; personalized measurements; acoustic virtual reality; visually impaired; transfer function measurement; hardware equalization

1. Introduction

The last decade has been a huge step forward in developing different types of electronic travel aids (ETA) with new capabilities. These ETAs benefit from different kinds of newly available technologies to assist the real world guidance of the visually impaired people. Many new ETAs have been designed and implemented with significant research efforts: NavBelt&GuideCane [1], Sounding Landscape [2], RFID [3], [4], SVETA [5], BlindAid [6], wireless sensor networks [7], iSONIC [8], CASBliP [9], eBox [10], Drishti [11], just a few to mention. A

[1] PhD student, Depart. of Applied Electronics, University "Politehnica" of Timişoara, Romania, e-mail: zoltan.haraszy@etc.upt.ro

recent survey of wearable obstacle avoidance ETAs for the blind is presented in [12]. These devices improve the mobility of the blind users, in terms of safety and speed, in unknown or dynamically changing environments.

In spite of the achievements no single ETA, designed until today, has been widely accepted by the community of the blind and visually impaired people. The success of ETAs is highly dependent on the proper man-machine interface (MMI) used between the blind subject and the system (how and what information is sent to the user). The Acoustic Virtual Reality (AVR) concept can be used successfully to design and implement such a MMI [13], [14]. The idea of such a human-computer interface (HCI) has been suggested by spatial sound source localization ability of the human hearing [15], and must be designed in such a way to be approved by the blind community.

The AVR concept proposes to exchange the visual reality with an appropriate acoustic virtual reality. The AVR is based on a few rules that are presented here:

- The presence of obstacles is signalized to the subject by burst of sounds, whose virtual source position suggests the position of real obstacles;
- Different obstacles are individualized by different acoustic signals (sounds);
- The intensity and the repetition frequency of the acoustic signals depend on the distance between the subject and obstacles;
- A pilot signal is used to indicate the direction of the movement to the target.

In order to obtain the corresponding acoustic signals for the left and right ears, whose virtual sound source suggests the presence of an existing obstacle to the visually impaired person, the Head Related Transfer Functions (HRTFs) can be used.

Basically, the HRTFs are mathematical representations of the influence of the human acoustic system, composed of the ear, the head and the torso, on the deformation of the acoustic signal's spectrum, which reaches the listener's ear coming from a particular direction of the 3D space. They represent a pair of two transfer functions (one for each ear) for each location in the 3D space. HRTFs not only vary with azimuth, elevation, frequency and distance to the sound source, but also vary significantly from person to person [16]. HRTFs are frequency domain functions, although the direct result of most HRTF measurements are the Head Related Impulse Responses (HRIRs), which are time domain equivalents of the HRTFs.

For each person, measured HRTFs are grouped in data sets, which include a high number of HRTFs measured in different directions. Considerable effort has been put into making HRTF databases available for scientific research. As a result

of these efforts, there are many publicly available HRTF databases: LISTEN [17], CIPIC [18], Kemar [19], and other databases.

HRTF measurements are almost always conducted in anechoic environments, such as anechoic chambers, although HRTF measurements in everyday environments are also reported in the literature [20]-[23]. The basic scenario is to transmit a known acoustic signal via a loudspeaker placed at azimuth θ, elevation φ and distance r from the listener's head, and record the filtered acoustic signals using binaural microphones placed at the entrance of the open/blocked ear canal or in the ear canal. Please note that all angles (azimuth and elevation) are given with respect to the vertical-polar coordinate system, which is the most commonly used coordinate system in the literature [24].

The current paper presents a feasible near anechoic measurement scenario for practical cases, where no such chamber is available. Compared to the most of the public databases, our intention is to obtain the HRTFs for directions in the horizontal plane with azimuth angles between -90 and +90 degrees. Also, measurements are conducted on a more densely spaced grid, which poses an advantage for the interpolation of HRTFs in AVR development.

The rest of the paper is organized as follows. Chapter II has two sections: the first presents the measurement facility and hardware. The second shortly explains the experimental procedure and control software. Chapter III describes the design of the test signal. In Chapter IV, the post-processing procedure used to extract HRTFs from the measured raw acoustic signals is presented. Chapter V explains the experimental results, while the last chapter is devoted to conclusions, possible improvements and future research plans.

2. HRTF Measurement

If someone wants to measure the HRTFs, there are two methods: one is called the direct method [17], [18], [19] and the other one is called the reciprocal method [25]. The direct method is to measure the HRTFs by broadcasting the test signal at different directions of the 3D space and recording the received acoustic signal at the entrance of the two ears. The other, reciprocal method is based on Helmholtz' principle of reciprocity, in which the place of the broadcasting and receiving end are exchanged. The measurement scenario, described in the current paper, is based on the direct method.

A. The Measurement Facility and Hardware

The measurement facility is presented in Fig. 1. Our experimental room was built at a local furniture factory, where plenty of foam was available. The walls were 3.2 meters long, 3 meters wide, at least 2 meters high and were constructed from thick foam with a minimum thickness of 0.6 meters. The floor was covered with foam with a thickness of 0.2 meters. The scope of this

experimental room was to create measurement conditions near to an anechoic chamber by reducing internal reflections and isolating outside noise. The speaker was placed on a table built from foam (0.75 meters x 0.6 meters) at the same height (1.1 meters from the ground) with the head to ensure the horizontal plane measurements. The table was placed near one of the foam walls, as can be seen in Fig. 1. The rotating chair was placed at approximately 2 meters from the loudspeaker in order to ensure that the distance between the sound source and the center of the head is equal to 2 meters, for a good approximation of the plane wave in the measuring points from the horizontal plane [26].

The measurement hardware configuration is shown in Fig. 2 and consists of the following components:

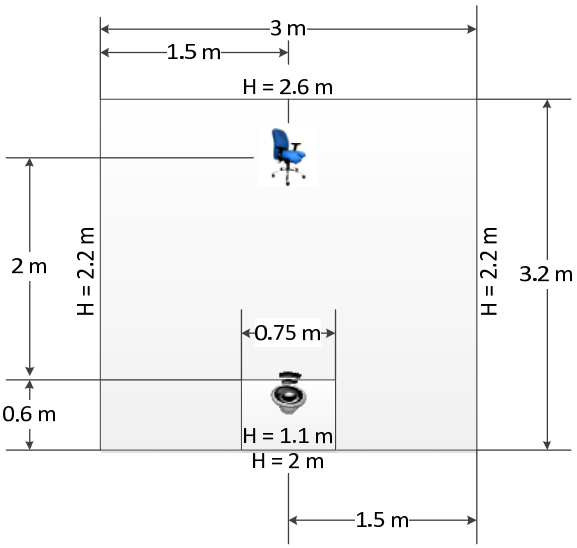

Fig. 1. The measurement facility. Please note that abbreviation H stands for the height of different walls and for the table.

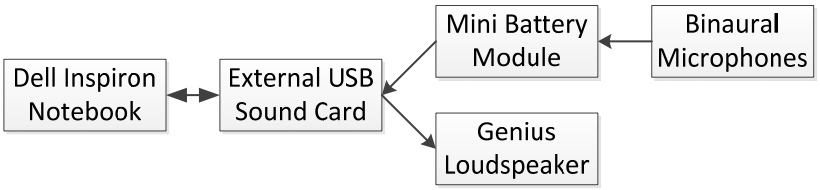

Fig. 2. The measurement hardware configuration.

- Dell Inspiron 1520 notebook running Windows 7 Ultimate 32-bit operating system, with National Instruments' LabVIEW guiding the whole measurement;

- Andrea Pureaudio USB-SA hi-fidelity external USB sound card powered via USB from the laptop. Communication with the laptop is implemented via USB. Ensures 2 channel stereo microphone input for the in-ear binaural microphones and 2 channel stereo audio output for the loudspeaker, with 3.5 mm jacks for both microphones and loudspeaker [27];
- Sound Professionals SP-SPSB-8 mini battery module with standard 9V battery, for improved high sound pressure level (SPL) performance. The battery module is connected to the USB sound card and to the in-ear microphones using Sound Professionals SP-SPSC-1 high quality stereo double shielded stereo extension cable;
- Sound Professionals SP-TFB-2-80015 low noise in-ear binaural microphones with standard sensitivity, used to record the binaural signals, which are mounted in extremely comfortable, in-ear holders that slip right into the ear structure. Foam windscreens (Sound Professionals SP-MINI-WS) were also used with the in-ear binaural microphones to ensure stable positioning of the microphones relative to the ear through the whole measurement, because even relative small positional changes in the capsule position alter notably the HRTF characteristics [28]. In our measurements the binaural microphones were place at the open ear canal entrance, where the results indicate that for most listeners HRTF measurements are of very high quality [29], although variation between subjects of HRTFs measured at the blocked ear canal is smaller than at the same point with open ear canal [30]. The windscreens are acoustically transparent to allow sound to pass through the ears and microphones completely unchanged;
- Genius SP-G16 stereo sound loudspeaker, with a frequency response between 20 Hz and 20 kHz, destined to transmit the measurement test signal.

B. Experimental Procedure and Software

As we mentioned earlier, the current experiments yielded HRTF data only at directions specified by azimuth angles between -90 and +90 degrees for elevation angle 0 degree. The resolution of our measurements was 5 degrees, which is the necessary angle between HRTFs in the horizontal plane [31], although [32] claims that spatial resolution of HRTF measurement positions can be reduced from 5 to about 10 degrees without introducing strong perceptual differences. This totals a number of 37 measurements for our test subject. The listener used a field compass placed horizontally between its legs for simple angle adjustment.

Before the actual measurement to begin, the measurement assistant has to correctly configure the graphical user interface (GUI), implemented in LabVIEW, by setting the parameters of the measurement signal. These parameters are presented in Chapter III. The measurement software, presented in Fig. 3, consists of a virtual instrument (VI).

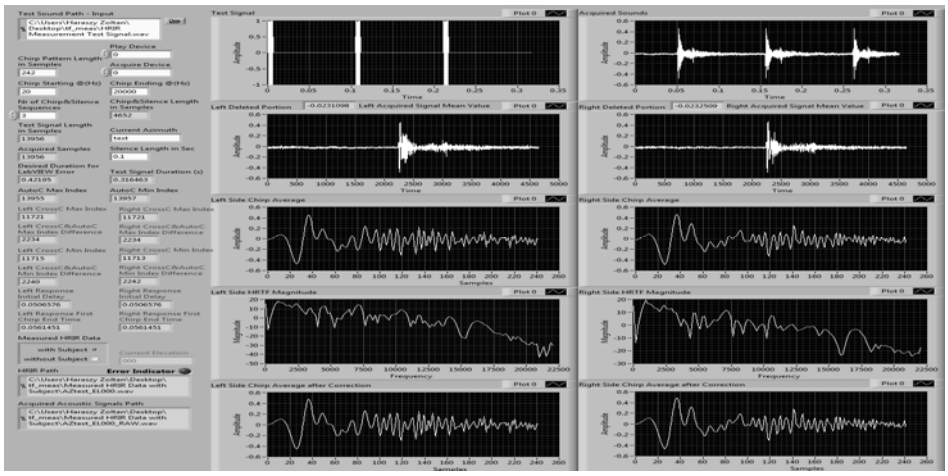

Fig. 3. A snapshot of the measurement software (GUI) implemented in LabVIEW graphical environment.

The measurement for one single direction is described as follows. In the first step, the test subject adjusts the position of the rotating chair to the desired direction, and second, the person assisting the whole measurement executes the VI. The two binaural signals recorded using the in-ear microphones are saved in Microsoft Wave (.wav) format on the HDD of the notebook for post-measurement extraction of the HRTF data from the raw measurement signals. This procedure is repeated for each of the 37 measurement directions.

Please note that the measurement from the current paper do not take into account the effect of the acoustical environment near to the head, such as the human hair.

Such a measurement system introduces its own filtering on the signal transmitted by the loudspeaker and, consequently, on the signal recorded by the binaural microphones. To eliminate this drawback, the recorded binaural signal must be post-measurement equalized. This will ensure faithful reproduction when using the measured HRTFs for spatial virtual audio reproduction.

To achieve correct equalization (compensation) for the recording signals, there are two methods that can be used.

The first method is to measure the reference responses for all the measurement directions. This type of compensation was used in [33] and [34]. During this procedure the whole system (loudspeaker, binaural microphones, etc.) work exactly as during any regular measurement, the only difference is that there is no listener seated in the rotating chair. By using this approach many negative effects, which lower measurement accuracy, can be limited:

- the influence of the measurement hardware's frequency and directivity responses are eliminated;

- the influence of the acoustic characteristics of the test room and the reflections from the device elements are significantly reduced.

The second method is to measure the impulse responses (IRs) of each device of the measurement system or to measure the IR of the whole measurement system, and after determining the inverse IR(s), to use them to equalize the raw HRTF data.

Currently, our measurement system is not able to precisely measure the reference responses for all the measurements directions, because we are not able to precisely position the binaural microphones in the same place as if the listener were present.

In conclusion, the first method cannot be used in our current measurements. Consequently, the second method, by measuring the whole measurement system's IR, is used to compensate for the influences of the measurement hardware configuration. Details of how this calibration is done are presented in Chapter IV.

3. Design of the test signal

Over the past century many different excitation signals have been developed to measure different transfer functions, such as impulses, maximum-length sequences, periodic signals of length 2^N, stepped sine and sweeps. Among these excitation signals, the optimal choice is using a sweep signal due many reasons. Sweeps can exclude all harmonic distortion products from IRs, practically leaving only background noise as the limitation for the achievable signal-to-noise ratio (SNR). The sweep can thus be fed with considerable more power to the speaker without introducing artifacts in the acquired IR. Sweep-based measurements are also significantly less vulnerable to the deleterious effects of time variance [35]. Unlike other methods, using sweeps does not necessitate a tedious calibration in order to obtain very good results and it is the best IR measurement technique in an unoccupied and quiet room [36].

In our experiments, the test signal is generated by LabVIEW. The standard chirp signal in LabVIEW is a linear sweep, which is already implemented. The linearly varying-frequency sine sweep can be mathematically described as (1):

$$x(t) = A\sin(f(t)) \tag{1}$$

The instantaneous frequency is given by the derivative of the argument of the sine function. If we assume a linearly varying frequency, starting from f_1 and ending to f_2 in the total time T, we obtain (2):

$$\frac{d(f(t))}{dt} = \omega_1 + \frac{\omega_2 - \omega_1}{T} t \tag{2a}$$

$$\frac{d(f(t))}{dt} = 2\pi \left(f_1 + \frac{f_2 - f_1}{T} \right) t \tag{2b}$$

which is satisfied, if we pose (3):

$$f(t) = \omega_1 t + \frac{\omega_2 - \omega_1}{T} \cdot \frac{t^2}{2} \tag{3a}$$

$$f(t) = 2\pi \left(f_1 t + \frac{f_2 - f_1}{T} \right) \cdot \frac{t^2}{2} \tag{3b}$$

The frequency of the chirp varies linearly in time from 20 Hz to 20 kHz. The sweep time of a single chirp depends on the distance between the loudspeaker and the head of the subject. As can be seen in Fig. 1, in our measurements, the distance is 2 meters. This means that the time for the chirp to travel from the loudspeaker to the microphone is about 5.83 ms (257 samples at a sample rate of 44.1 kHz), considering the speed of sound at 343.2 m/s. In order to avoid an overlap between the reflections caused by our test subject and the reflections caused by surrounding walls or other equipment, we decided to use a total of 242 samples for our chirp, which is equivalent with a chirp duration of about 5.49 ms. Thus, there were a total of 242 samples at a sample rate of 44.1 kHz. A similar approach is used in [33], where the chirp signal is filtered with a FIR filter in order to enhance the magnitude of the lower frequencies in order to improve SNR [35] and leave other frequencies untouched.

The stimulating chirp signal is repeated several times in order to average the system response in the time domain. This way, the SNR of the measured signals can be improved. Because the system responses will be used for convolution with real signals, they cannot be too long. Moreover, if they were too long, they would extend the measurement times. Also, by using such a test signal, data acquisition input and output channels have to be triggered once for every measurement direction, which avoids losing synchronization caused by the starting up and closing down different devices many times.

In our measurements, the test signal was composed of 10 chirp and silence sequences of the same length concatenated one of another. Fig. 4 shows the chirp signal in time domain. As we mentioned, the chirp signal was 242 samples long. The silence between the chirps was 0.3 seconds long to ensure that the possible reverberant echoes die out, which means 13230 samples long at a sample rate of 44.1 kHz. Consequently, the test signal, shown in Fig. 5, including 10 chirp and

silence sequences, is 134720 samples long, which means about 3.05 seconds at a sampling rate of 44.1 kHz.

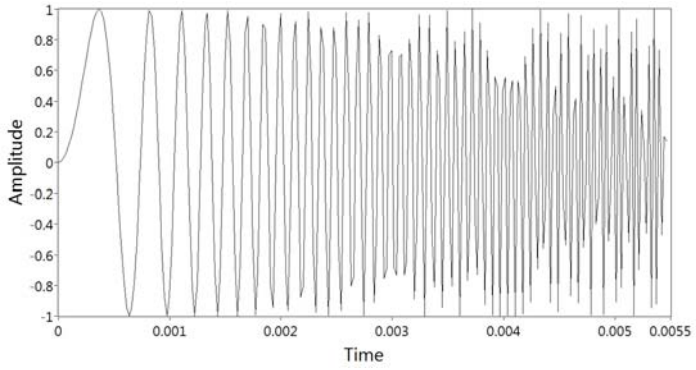

Fig. 4. Chirp signal in time domain.

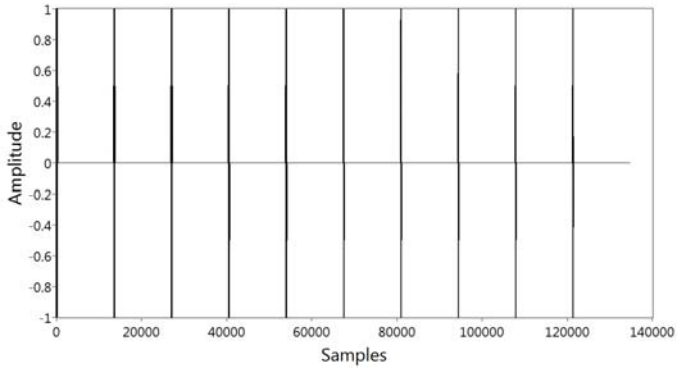

Fig. 5. The test signal used in our experiments, consisting of a total of 10 chirp and silence sequences.

All the measurement parameters, like starting frequency, ending frequency, silence length, number of chirp and silence sequences, are set from the designed LabVIEW interface.

4. Post-measurement processing for HRTF data extraction

We presented the design of the test signal in the previous chapter. For each of the 37 measurement positions, we recorded two raw acoustic signals, which are filtered versions of our test signal and include all the important HRTF data. The length in samples for each of these two signals is 134718.

This chapter contains a detailed description of how the compensated HRTF data is determined. The following procedure is valid for both (left and right) channels.

In the first step, we must calculate the average of recorded individual chirp signals after extracting them from the recorded raw signals. Second, we determine from the average chirp signals the non-compensated HRTF data. In the third step, the measurement system's inverse impulse response must be calculated in order to compensate the previously obtained HRTF data. Last, we determine the equalized HRTF data using the results obtained following the second and third steps.

All the post-measurement processing is implemented using a VI developed in LabVIEW.

A. Determine the average chirp signal

The whole procedure of determining the average chirp signal from the raw signal is presented in Fig. 6.

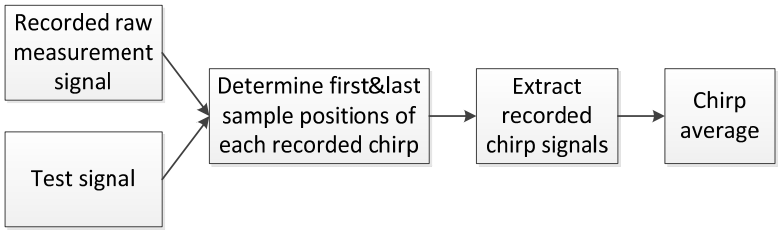

Fig. 6. Obtaining the average chirp signal from the raw measurement signal and the test signal.

In order to correctly extract the received chirp signals from the raw measurement signal, we must precisely determine where those chirps are positioned inside the raw signal. To obtain the position of the first sample of the first recorded chirp, we determine the minimum between the following two values:

- the difference between the position where the maximum value of the test signal's autocorrelation is located and the position where the maximum value of the cross-correlation, between the test signal (10 chirp and silence sequences) and the recorded raw signal, is situated;
- the difference between the position where the maximum value of the test signal's autocorrelation is located and the position where the minimum value of the cross-correlation, between the test signal (10 chirp and silence sequences) and the recorded raw signal, is situated.

To obtain the position of the last sample of the first chirp, we add the sample length of a single chirp to the resulting minimum value, which gives us the position of the first sample of the first chirp. Once we know where the first recorded chirp is situated, we can determine the other chirps' first and last sample

positions by adding to these values the sample length of a single chirp and silence sequence, which in our case is 13230. Now, having determined each of the 10 recorded chirps is positioned, we can extract them and calculate their average, called chirp average.

Please note that the relative positions of the first chirp's first sample for both channels can be used to determine the received chirps' arrival time. The difference between these arrival times enables us to determine the Interaural Time Difference between the recorded chirps, which is a major localization cue at low frequencies [37].

B. Determine the non-compensated HRTF data

The whole process of calculating the non-compensated HRTF data from one single input chirp and the obtained chirp average, as a result of the first processing step, is presented shown in Fig. 7.

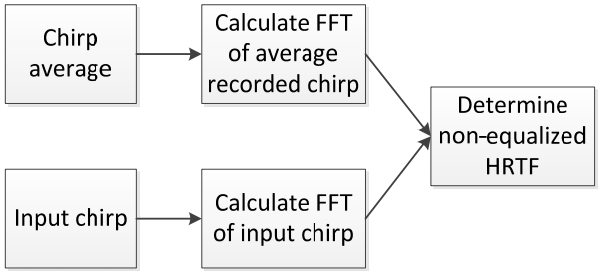

Fig. 7. Determining the non-equalized HRTF from the chirp average and the input chirp.

To calculate the non-equalized HRTF:

- we transform into frequency domain both the chirp average and the input chirp;
- we perform a frequency domain division on the resulting frequency domain signals.

C. Determine the inverse impulse response of the measurement system

The steps for calculating the measurement system's inverse IR are depicted in Fig. 8.

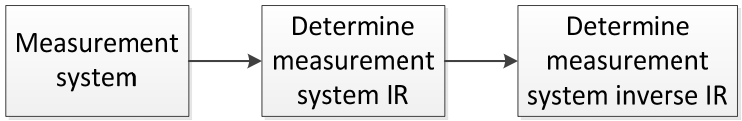

Fig. 8. Calculating the measurement system's inverse IR.

First, in order to calculate the measurement system's inverse IR, we must determine the system's IR (Fig. 9). We used the transfer function measurement

toolbox developed in frame of the RealSimple project [38] and measured the whole system's IR using the Golay code procedure by placing each of the microphones at a 2 cm distance from the loudspeaker, as seen in Fig. 10. The hardware configuration remained the same as described in Chapter II and depicted in Fig. 2. Fig. 9 depicts the left channel transfer function's magnitude in frequency domain. The results for the right audio channels are very similar. After both IRs are known, we determine the inverse IRs by using the MATLAB scripts provided by B. Gardner in [19].

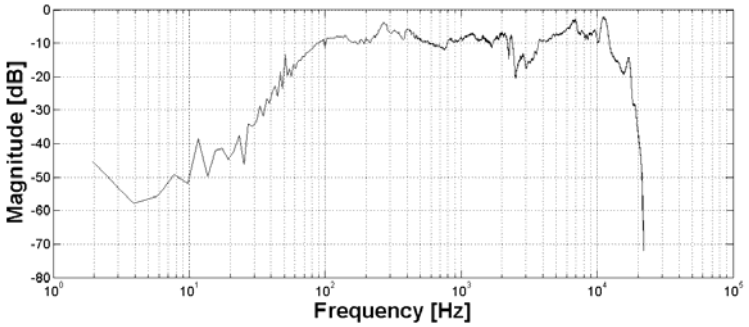

Fig. 9. Left channel transfer function of the measurement system.

D. Determine the compensated HRTF data

The method used in this paper for obtaining the equalized HRIR (time domain HRTF) from the non-equalized HRTF and the measurement system's inverse IR, the result of the third processing step, is presented in Fig. 10.

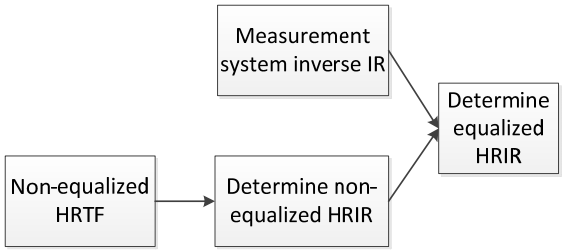

Fig. 10. Calculating the equalized HRIR from the non-equalized HRTF and the measurement system's inverse IR.

We obtained the non-equalized HRTF as the result of the second step. By applying the inverse FFT to it, we determine the non-equalized HRIR. Now, we use the system's inverse IR, result of the third processing step, and the non-equalized HRIR to determine the equalized HRIR obtained by the convolution of

these two extents, which is what we want to obtain as final result of all post-measurement processing.

5. Results

After post-processing our measured data as described in the previous chapter, we obtained 37 HRIRs for both audio channels (a total of 37x2 HRIRs), corresponding to 37 measurement directions in the horizontal plane (at elevation 0 degrees) with azimuth angles between -90 and +90 degrees with a 5 degree angular increment between the measurements.

6. Conclusions

In the current paper, we described in detail our HRTF measurement procedure, beginning with the measurement facility, hardware scenario, experimental procedure, and control software, through the design of the test signal, post-measurement processing and results.

We conclude that the measurement of the HRTFs in near anechoic environments is feasible. This fact ensures that the proposed measurement setup is much more cost effective. A modified version of our interpolation procedure will be applied on the obtained HRIRs in order to generate any HRIRs in the horizontal plane between the values of -90 and +90 degrees of azimuth. After interpolating the solution will be used for spatial virtual audio reproduction as part of a prototype ETA being designed for visually impaired people.

As future improvements of the current measurement scenario:

- we want to update our measurement setup in order to be able to use the first method described for compensation of the HRTF data against the effect of the measurement hardware and room influences;
- we want to produce a slight change in our test signal. We intend to use in place of the currently used linear chirp an exponential sweep, motivated by an exponentially increasing sweep rate to provide more time and energy at low frequencies than the traditional linear sine sweep, among other advantages [39]. Also, a change is the starting and ending frequencies is possible depending on the measurements systems IR;
- we want to include a headrest on the chair to ensure a stable head position during the measurements, because HRTFs measured without using head-support aids are likely to have a high margin of error caused by head movements [39]-[42];
- we want to improve our measurement scenario to eliminate the drawback of only being able to measure HRTFs in the horizontal plane and to be able to measure HRTFs in any desired direction;

- we want to perform a new set of HRTF measurements, because our current measurement were performed with the microphones placed at the open ear canal, but the blocked entrance is the most suitable point for measurements of HRTFs and for binaural recordings, since sound at this point includes the complete spatial information, and in addition to that the minimum amount of individual information [43]. Measurements at the entrance of the blocked ear canal are validated in [44], which are usually performed. This will make it possible to compare the two HRTF measurements.

Acknowledgments

This work was partially supported by CNCSIS – UEFISCDI PNII – IDEI Grant Contract No. 599/19.01.2009.

R E F E R E N C E S

[1] *S. Shoval, I. Ulrich, J. Borenstein*, "Robotics-based Obstacle Avoidance Systems for the Blind and Visually Impaired", Invited article for the IEEE Robotics and Automation Magazine, Special Issue on Robotics in Bio-Engineering, **vol. 10**, n. 1, March 2003, pp. 9-20.

[2] *F. Fontana, A. Fusiello, M. Gobbi, V. Murino, D. Roccheso, L. Sartor, A. Panuccio*, "A Cross-Modal Electronic Travel Aid Device", In F. Paterno (Ed.), Mobile HCI (Berlin: Springer-Verlag, 2002, 393-397).

[3] *V. Kulyukin, C. Gharpure, J. Nicholson, S. Pavithran*, "RFID in Robot-Assisted Indoor Navigation for the Visually Impaired", 2004 IEEE/RSJ International Conference on Intelligent Robots and Systems (IROS 2004), September 28 - October 2, 2004, Sendai, Japan.

[4] *S. Carcieri, S. Morris, B. D. Perry*, "RFID Technology to Aid in Navigation and Organization for the Blind and Partially Sighted", B. Sc. Thesis, Worcester Polytechnic Institute, Copenhagen, Denmark, 2009.

[5] *G. Balakrishnan, G. Sainarayanan, R. Nagarajan, S. Yaacob*, "Wearable Real-Time Stereo Vision for the Visually Impaired", Engineering Letters, **vol. 14**, n. 2, May 2007, pp. 6-14.

[6] *S. Mau, N. Melchior, M. Makatchev, A. Steinfeld*, "BlindAid: An Eletronic Travel Aid for the Blind", The Robotics Institute, Carneggie Mellon University, Pittsburgh, May 2008.

[7] *K. Beydoun, V. Felea, H. Guyennet*, "Wireless sensor network system helping navigation of the visually impaired", Information and Communication Technologies: from Theory to Applications (ICTTA'08), 2008, Damascus, Syrian Arab Republic.

[8] *L. Kim, S. Park, S. Lee, S. Ha*, "An electronic traveler aid for the blind using multiple range sensors", IEICE Electronic Express, **vol. 6**, n. 11, June 2009, pp. 794-799.

[9] *G. P. Fajarnes, L. Dunai, V. S. Praderas, I. Dunai*, "CASBliP – a new cognitive object detection and orientation system for impaired people", 4th International Conference on Cognitive Systems, CogSys 2010, January 27-28, 2010, Zurich, Switzerland.

[10] *A. Kumar, R. Patra, M. Manjunatha, J. Mukhopadhyay, A. K. Majumdar*, "An electronic travel aid for navigation of visually impaired persons", 3rd International Conference on Communication Systems and Network (COMSNETS 2011), January 4-8, 2011, Bangalore, India.

[11] A. *Helal, S. E. Moore, B. Ramachandran*, "Drishti: An Integrated Navigation System for Visually Impaired and Disabled", 5th IEEE International Symposium on Wearable Computers (ISWC'01), October 7-9, 2011, Zurich, Switzerland.

[12] *D. Dakopoulos, N. G. Bourbakis*, "Wearable Obstacle Avoidance Electronic Travel Aids for Blind: A Survey", IEEE Transactions on Systems, Man, and Cybernetics – Part C: Applications and Reviews", **vol. 40**, n. 1, January 2010, pp. 25-35.

[13] *V. Tiponut, A. Gacsadi, L. Tepelea, C. Lar, I. Gavrilut*, "Integrated Environment for Assisted Movement of Visually Impaired", 15th International Workshop on Robotics in Alpe-Adria-Danube Region (RAAD 2006), June 15-17, 2006, Balatonfured, Hungary.

[14] *V. Tiponut, Z. Haraszy, D. Ianchis, I. Lie*, "Acoustic Virtual Reality Performing Man-machine Interfacing of the Blind", 12th WSEAS International Conference on SYSTEMS, July 22-24, 2008, Heraklion, Greece.

[15] *J. Blauert*, "Spatial Hearing – The Psychophysics of Human Sound Localization", Revised Edition (The MIT Press, 1997).

[16] H. *Moller, M. F. Sorensen, C. B. Jensen, D. Hammershoi*, "Binaural Technique: Do We Need Individual Recordings?", The Journal of Audio Engineering Society, **vol. 44**, n. 6, June 1996, pp. 451-469.

[17] *Ircam, AKG Acoustics*, "LISTEN HRTF Database", http://www.ircam.fr/equipes/salles/listen/index.html, 2002.

[18] *V. R. Algazi, R. O. Duda, D. M. Thompson, C. Avendano*, "The CIPIC HRTF Database," 2001 IEEE Workshop on Applications of Signal Processing to Audio and Electroacoustics, October 21-24, 2001, Mohonk Mountain House, New Paltz, New York, USA.

[19] *W.G. Gardner, K.D. Martin*, "HRTF measurements of a KEMAR", The Journal of the Acoustical Society of America, **vol. 97**, n. 6, June 1995, pp. 3907-3908.

[20] *J. S. Abel, S. H. Foster*, "Measuring HRTFs in a Reflective Environment", 2nd International Conference on Auditory Displays (ICAD'94), November 7-9, 1994, Santa Fe, New Mexico, USA.

[21] *S. Takane*, "Estimation of HRIRs from impulse responses measured in ordinary sound field", International Workshop on the Principles and Applications of Spatial Hearing 2009 (IWPASH 2009), November 11-13, 2009, Zao, Miyagi, Japan.

[22] *Q. Ye, Q. Dong, Y. Zhang, X. Li*, "Fast Head-Related Transfer Function Measurement in Complex Environments", 20th International Congress on Acoustics (ICA 2010), August 23-27, 2010, Sydney, Australia.

[23] *M. Durkovic, F. Sagstetter, K. Diepold*, "HRTF Measurements With Recorded Reference Signal", 129th Audio Engineering Society Convention, November 4-7, 2010, San Francisco, California, USA.

[24] *M. Teschl*, "Binaural Sound Reproduction via Distributed Loudspeaker Systems", BSc dissertation, Institute of Electronic Music and Acoustics, Graz, Austria, 2000.

[25] *D. N. Zotkin, R. Duraiswami, E. Grassi, N. A. Gumerov*. "Fast head-related transfer function measurement via reciprocity", The Journal of the Acoustical Society of America, **vol. 120**, n. 4, October 2006, pp. 2202–2215.

[26] *M. Otani, T. Hirahara*, "Numerical study on source-distance dependency of head-related transfer functions", The Journal of the Acoustical Society of America, **vol. 125**, n. 5, May 2009, pp. 3253–3261.

[27] *Andrea Electronics Corporation*, "Pureaudio USB-SA Hi-Fidelity External USB Sound Card Spec Sheet", http://www.andreaelectronics.com/pdf_files/ProductSpecs/USB-SASpec.pdf, 2011.

[28] *K. A. J. Riederer*, "Part IIIa: Effect of microphone position changes on blocked cavum conchae head-related transfer functions", 18th International Congress on Acoustics (ICA 2004), April 4-9, 2004, Kyoto, Japan.

[29] *F. L. Wightman, D. J. Kistler, S. H. Foster, J. Abel*, "A Comparison of Head-Related Transfer Functions Measured Deep in the Ear Canal and at the Ear Canal Entrance", 18th Midwinter Meeting of the Association for Research in Otolaryngology, 1995, St. Petersburg Beach, Florida, USA.

[30] *H. Moller, M. F. Sorensen, D. Hammershoi, C. B. Jensen*, "Head-Related Transfer Functions of Human Subjects", The Journal of Audio Engineering Society, **vol. 43**, n. 5, May 1995, pp. 300-321.

[31] *T. Ajdler, C. Faller, L. Sbaiz, M. Vetterli*, "Interpolation of the Head Related Transfer Functions Considering Acoustic", 118th Audio Engineering Society Convention, May 28-31, 2005, Barcelona, Spain.

[32] J. *Breebaart, F. Nater, A. Kohlrausch*, "Spectral and Spatial Parameter Resolution Requirements for Parametric, Filter-Bank-Based HRTF Processing", The Journal of Audio Engineering Society, **vol. 58**, n. 3, March 2010, pp. 126-140.

[33] *M. Zhang, W. Zhang, R. A. Kennedy, T. D. Abhayapala*, "HRTF measurement on KEMAR manikin", Acoustics 2009, November 23-25, 2009, Adelaide, Australia.

[34] *A. Dobrucki, P. Plaskota, P. Prucknicki, M. Pec, M. Bujacz, P. Strumillo*, "Measurement System for Personalized Head-Related Transfer Functions and Its Verification by Virtual Source Localization Trials with Visually Impaired and Sighted Individuals", The Journal of Audio Engineering Society, **vol. 58**, n. 9, September 2010, pp. 724-738.

[35] *S. Müller, P. Massarani*, "Transfer-Function Measurement with Sweeps", The Journal of Audio Engineering Society, vol. 49, n. 6, June 2001, pp. 443-471.

[36] *G.-B. Stan, J.-J. Embrechts, D. Archambeau*, "Comparison of Different Impulse Response Measurement Techniques", The Journal of Audio Engineering Society, **vol. 50**, n. 4, April 2002, pp. 249-262.

[37] *F. L. Wightman, D. J. Kistler*, "The dominant role of low-frequency interaural time differences in sound localization", The Journal of the Acoustical Society of America, **vol. 91**, n. 3, March 1992, pp. 1648-1661.

[38] *E. J. Berdahl, J. O. Smith*, "Transfer function measurement toolbox", June 2007, http://ccrma.stanford.edu/realsimple/imp_meas/.

[39] *A. Farina*, "Simultaneous Measurement of Impulse Response and Distortion with a Swept-Sine Technique", 108th Audio Engineering Society Convention, February 19-22, 2000, Paris, France.

[40] *K. A. J. Riederer*, "Part Va: Effect of Head Movements on Measured Head-Related Transfer Functions", 18th International Congress on Acoustics (ICA 2004), April 4-9, 2004, Kyoto, Japan.

[41] *T. Hirahara, D. Morikawa, M. Otani*, "Effect of Head Movement in HRTF Measurements", International Workshop on the Principles and Applications of Spatial Hearing 2009 (IWPASH 2009), November 11-13, 2009, Zao, Miyagi, Japan.

[42] *T. Hirahara, H. Sagara, I. Toshima, M. Otani*, "Head movement during head-related transfer function measurement", Acoustical Science and Technology, **vol. 31**, n. 2, March 2010, pp. 165-171.

[43] *D. Hammershoi, H. Moller*, "Sound transmission to and within the human ear canal", The Journal of the Acoustical Society of America, **vol. 100**, n. 1, July 1996, pp. 408-427.

[44] *V. R. Algazi, C. Avendano, D. Thompson*, "Dependence of Subject and Measurement Position in Binaural Signal Acquisition", The Journal of Audio Engineering Society, **vol. 47**, n. 11, November 1999, pp. 937-947.